

Growth of GaAs Epitaxial Over Layer on SiO₂ Patterned Si Substrate for Laser Diode Fabrication

4.1 Introduction

Though there are many attempts to reduce the threading dislocations in GaAs epitaxial films on Si, there is a long way to achieve an improvement in the quality of GaAs on Si. Patterned epitaxy such as, selective area growth¹ or epitaxial lateral overgrowth (ELO)² over insulator³ or metallic⁴ masked substrate has a potential to use in the realization of various opto-electronic integrated circuits (OEICs). This method allows to grow single crystalline thin films on masked crystalline substrates by seeding through the seed openings. The growth of the ELO layers starts selectively in mask-free seeding areas and proceeds laterally over the mask film. If the growth allowed to go on for a sufficient time, the growth fronts from adjacent openings merge to form a continuous GaAs layer with the same orientation as the substrate.

Conventionally, in the lattice-mismatched system the dislocations caused by the relaxation of the buffer layer, propagate into the subsequently deposited structure and thus degrade device properties. In ELO technique part of the ELO epilayers grown on lattice mismatched substrates demonstrates nearly defect-free characteristics and it is highly suitable for device fabrication^{5,6}. This type of patterned epitaxy of GaAs films on Si substrates is a promising way to realize monolithic cointegration of GaAs devices on Si⁷.

Though dislocation blocking and confining by lateral growth appears conceptually very attractive and some devices have been fabricated by several groups^{8,9}, this ELO approach suffers from drawbacks due to the fact that the thickness of the GaAs overgrown film cannot be chosen independently from its

lateral extension¹⁰. However, attempts have been taken by different groups to optimize the so-called width to thickness ratio for the ELO film^{11,12}.

In this chapter, the growth of ELO layer on Si and the fabrication of GaAs quantum well (QW) laser on a patterned substrate has described. For the fabrication of laser, the mask space has chosen as 50 μm with 20 μm window region.

4.2 Experimental

4.2.1 Epitaxial growth of ELO layer

Figure 4.1 shows the schematic diagram of lateral epitaxial overgrowth of GaAs layer on SiO_2 mask with striped window openings on GaAs/Si. In the present study, prior to the ELO growth, 1 μm thick n^+ -GaAs buffer layer was deposited on a (100) n^+ -Si substrate with 5 times TCA and the substrate was masked by 100 nm thick SiO_2 deposited by radio frequency (rf) sputtering. In order to find out the 3D growth plane of GaAs on Si, star-like pre-patterning was done by photo-lithography on the SiO_2 mask. The identified growth plane was further used to optimize the ELO GaAs epitaxy using various stripe patterns. The overgrowth was carried out by controlling the growth rate with gradual change of growth temperature and flow rate of carrier gas. Post-growth annealing was done at 500 $^\circ\text{C}$ for 10 minutes after the ELO overgrowth of 1 μm thick n^+ -GaAs layer.

4.2.2 Fabrication of laser structure

To study the suitability of ELO GaAs layer quality on the lasing behavior of laser diode two type of structures were followed. The position of the top p^+ -GaAs and metal contact was used to differentiate the Type I and Type II laser

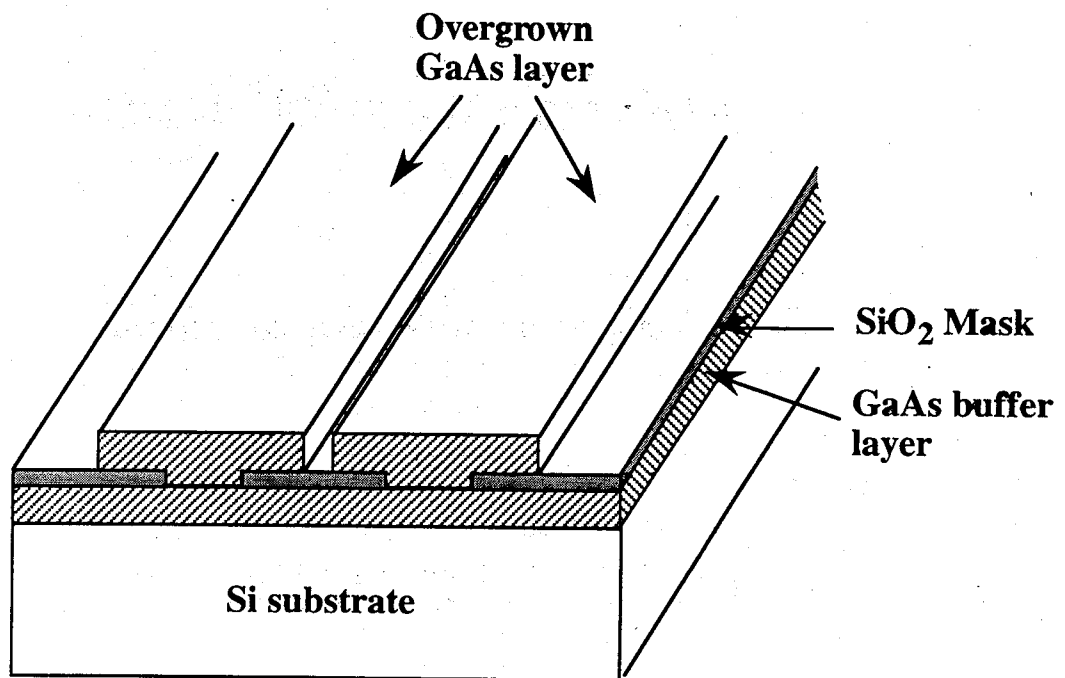


Figure 4.1 : Schematic diagram showing lateral epitaxial overgrown of GaAs layer on SiO₂ mask on a Si substrate.

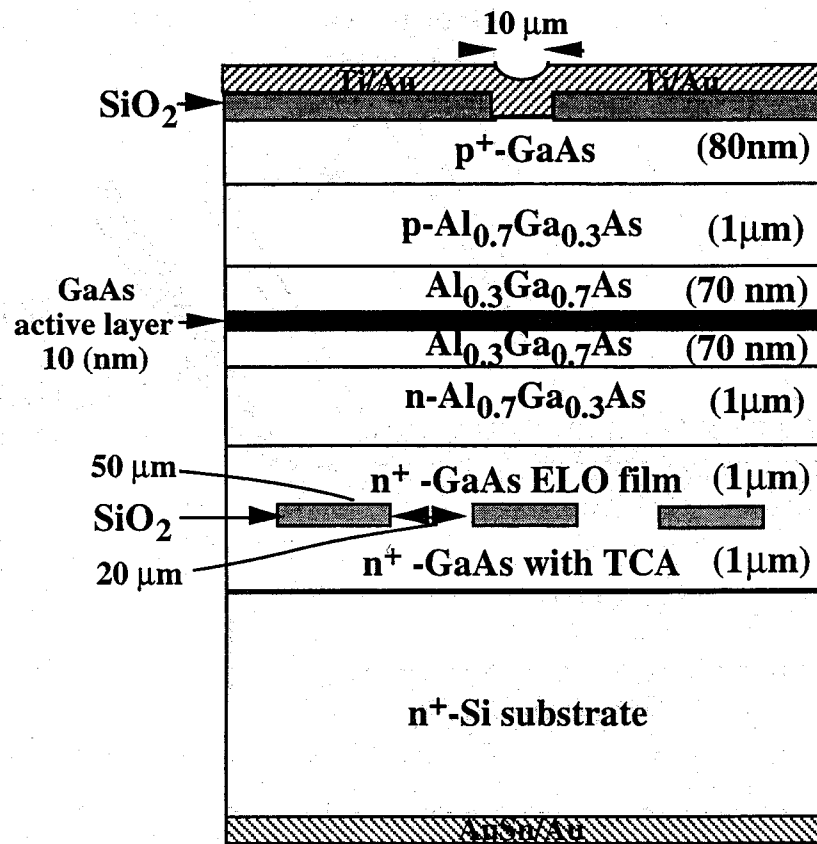


Figure 4.2 (a): Schematic structure of the MOCVD grown GaAs SQW laser (Type I) on a micro-channel patterned Si substrate.

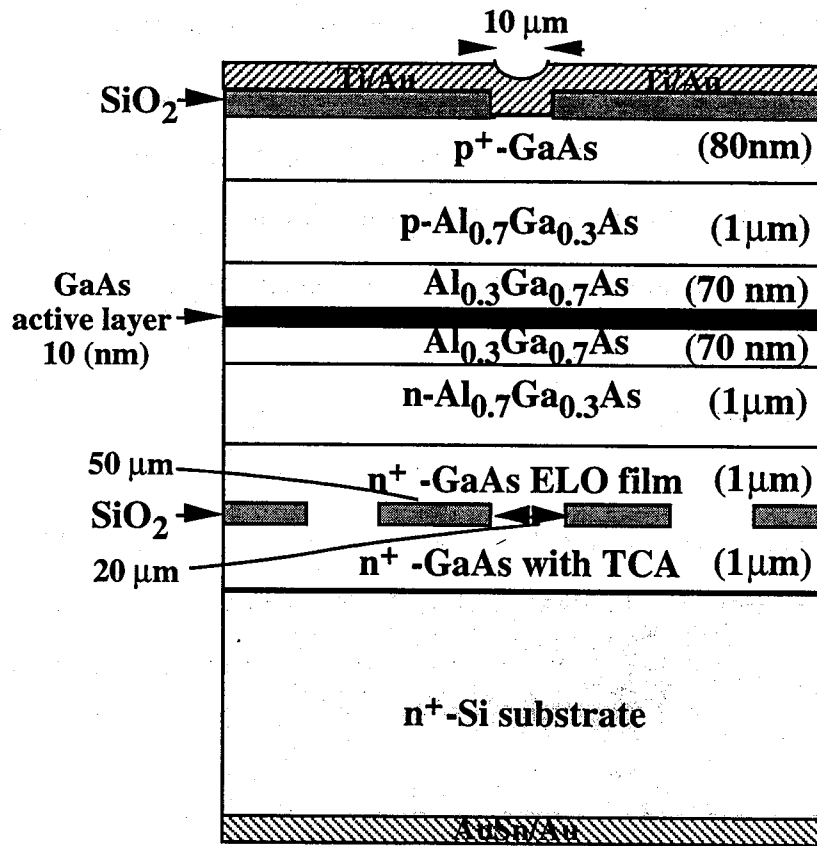


Figure 4.2 (b): Schematic structure of the MOCVD grown GaAs SQW laser (Type II) on a micro-channel patterned Si substrate.

diode structures. Type I laser diode was fabricated using the p^+ window layer in-line with the ELO layer in such a way to study the dislocation free active region. Type II laser diode was realized using the p^+ window layer in-line with the line seed region. Figure 4.2 (a) and Fig. 4.2(b) show the schematic structure of the MOCVD-grown AlGaAs/GaAs SQW type I and Type II laser diode respectively on Si with an ELO buffer layer. The laser diode structure consisted of a 1.0 μm thick $n\text{-Al}_{0.7}\text{Ga}_{0.3}\text{As}$ lower cladding layer, a 70 nm thick undoped $\text{Al}_{0.3}\text{Ga}_{0.7}\text{As}$ lower confining layer, a 10 nm thick undoped GaAs SQW active region, a 70 nm thick undoped $\text{Al}_{0.3}\text{Ga}_{0.7}\text{As}$ upper confining layer, a 1.0 μm thick $p\text{-Al}_{0.7}\text{Ga}_{0.3}\text{As}$ upper cladding layer and an 80 nm thick $p^+\text{-GaAs}$ contact layers.

4.2.3 Characterization studies

Optical microscope was used to check the surface morphology of the GaAs ELO layer on GaAs/Si. Molten KOH was used as the etchant to observe the etch pit density (EPD) on the ELO film. A 6 μm GaAs ELO layer was grown to carry out the etching experiment. Photoluminescence (PL) Scanning electron Microscope (SEM) was used to observe the interface properties of GaAs seeded ELO layer with SiO_2 mask.

Injected current vs. output light ($I\text{-}L$) characteristics were carried out to observe the lasing property of the ELO laser diodes. Automatic power controlled (APC) lifetime measurements have been performed in order to know the details on the degradation mechanism of laser diodes. Electron beam induced current (EBIC) measurements have been carried out in order to investigate the qualitative and quantitative information about the dislocation density by the dark spot density of EBIC image.

4.3 Results and discussion

4.3.1 Properties of ELO films

The primary problem in the ELO technique is that the formation of polycrystalline structure on the masked region. Usually the single crystalline epitaxial films are formed only on the exposed area of crystalline substrate. Areas covered with non-crystalline films (SiO_2) result in the growth of polycrystalline films. If the nucleation of GaAs on the masked surface takes place, it leads to the growth of polycrystalline epitaxial film over the masked area. On the other hand if the nucleation is controlled only inside the seed through, the GaAs grows vertically to the mask level and then laterally expand over the mask and which leads to the single crystalline ELO epitaxy. In the preliminary studies, it was observed that below 750°C lateral growth decreases because of the polycrystalline GaAs deposits and therefore low flow rates and high deposition temperature is required to suppress GaAs nucleation on the mask. The vertical growth through seed opening was carried out at a growth temperature of 850°C and then a gradual decrease in temperature with an interval of 20°C was done up to 750°C . The gradual decrease in growth temperature controls lateral-to-vertical growth velocity ratio (ELO ratio) homogeneously. ELO ratio found increased as growth temperature is decreased.

Figure 4.3 shows a photograph of an ELO sample which was grown from a star-like seed pattern with a line opening interval of 15° . The seed width opening was selected as $10\text{ }\mu\text{m}$. The ELO growth depending upon the seed orientation aligned can be viewed on (100) plane. It can be seen that the width of ELO was the largest when the stripe was 15° and 30° off-oriented from $\langle 110 \rangle$ and $\langle 010 \rangle$ directions or their equivalent directions, while the growth was vertical, when the stripe was oriented almost exactly in the $\langle 110 \rangle$ and $\langle 010 \rangle$ directions or their equivalent directions. The stripe patterns 15° -oriented from the $\langle 110 \rangle$ direction

was chosen for the further optimization of ELO ratio in order to overcome the difficulties associated with a very low lateral growth rate.

Further, the seed windows (3, 10, 20 μm) were oriented at 15° off from the $\langle 110 \rangle$ direction with the parallel spacing of 290, 160, 90 and 50 μm were used to optimize the ELO overgrowth with complete epitaxial layer. The correspondence of the seed width and lateral over growth rate was obtained.

Figures 4.4a and 4.4b show the surface morphology of optical micrograph of ELO film grown on SiO_2 pre-patterned Si substrate with the seed line opening width of 10 and 20 μm respectively. The seed line openings are spaced by 90 μm SiO_2 masked intervals. A 2 μm vertical growth on 10 μm seed opening resulted 30 μm lateral spread at 850°C for 20° step cooling. Whereas the lateral spread was 40 μm in the case of 20 μm seed opening. However, the total coverage can be achieved by increasing the thickness of the ELO film even for 90 μm mask interval. A decrease in the SiO_2 mask width influences surface morphology more smooth and result mirror like surface. In our case uniform, flat surface was obtained for a seed window opening of 20 μm with a space interval of 50 μm as shown in Fig. 4.5 at a ELO thickness 1 μm . It is important to obtain the smooth and complete layer at a reduced thickness in order to avoid the dead layer accumulation in-between the Si substrate and GaAs device, since this ELO layer is used as a buffer layer for defect reduction.

Figures 4.6 shows the cross sectional SEM image of the ELO film around the seed line opening of 20 μm with a space interval of 50 μm . It can be seen that the GaAs initially grow vertically and as soon as the growth over line seed gap complete starts to spread laterally over the SiO_2 without any polycrystalline domains.

To study the dislocations in ELO layers, etching experiments were carried out at 350°C for 10-12 min by molten potassium hydroxide (KOH). Fig. 4.7 shows the etch pit population. The etch pit was observed only in the region opened for vertical growth and the laterally grown layer is completely etch pit

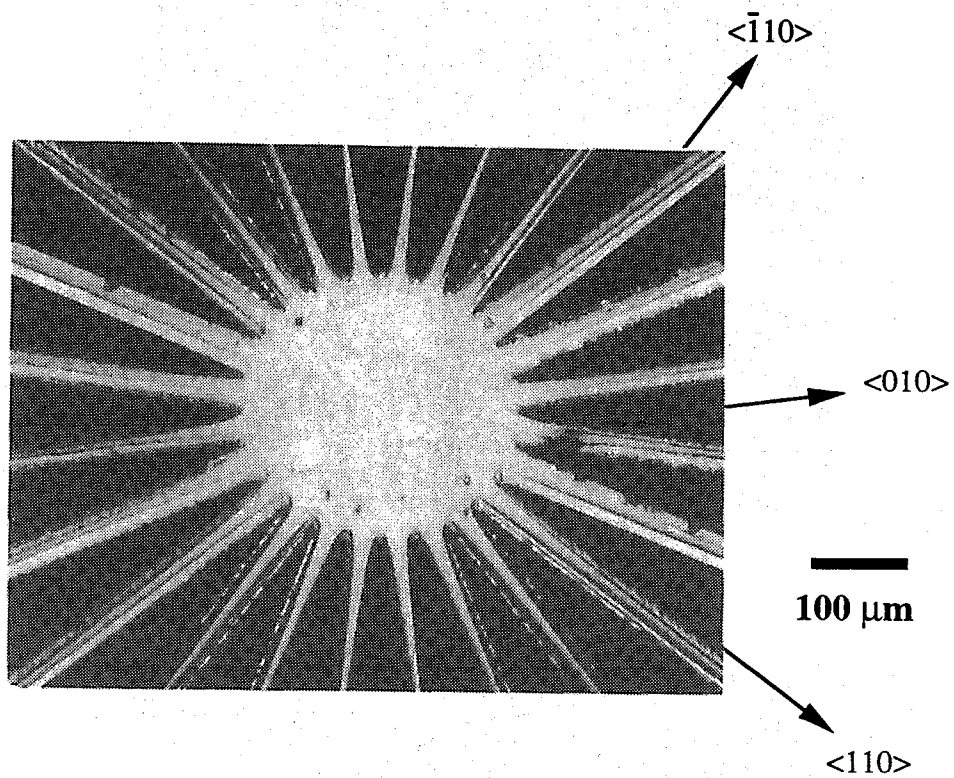
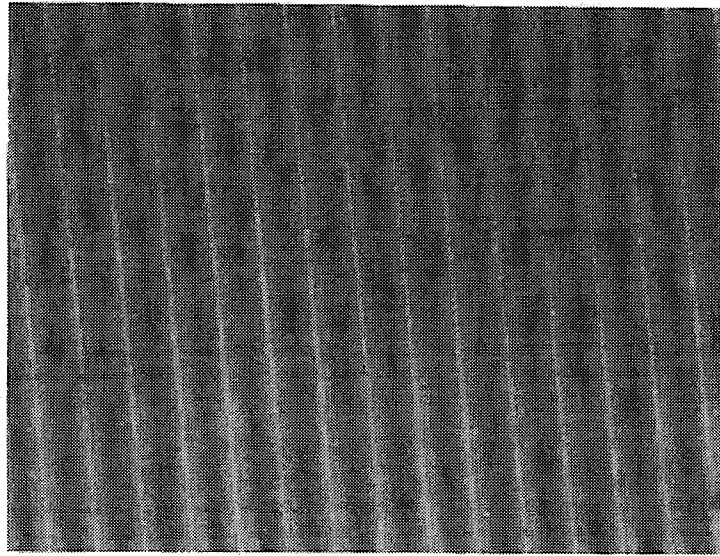
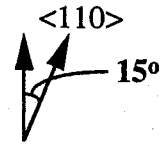
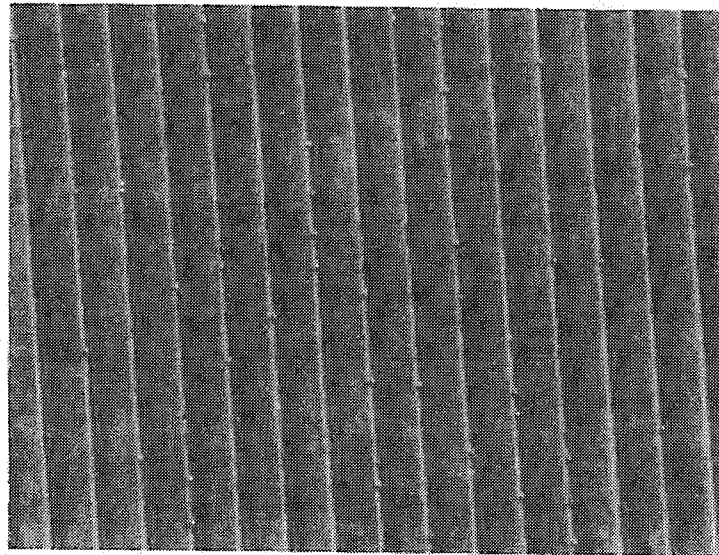


Figure 4.3 : ELO film on a star-like seed pattern on GaAs/Si.



200 μm

(a)



200 μm

(a)

Figure 4.4 : Surface morphology of optical micrograph of ELO film grown on SiO_2 pre-patterned Si substrate with the seed line opening width of (a) 10 μm and (b) 20 μm .

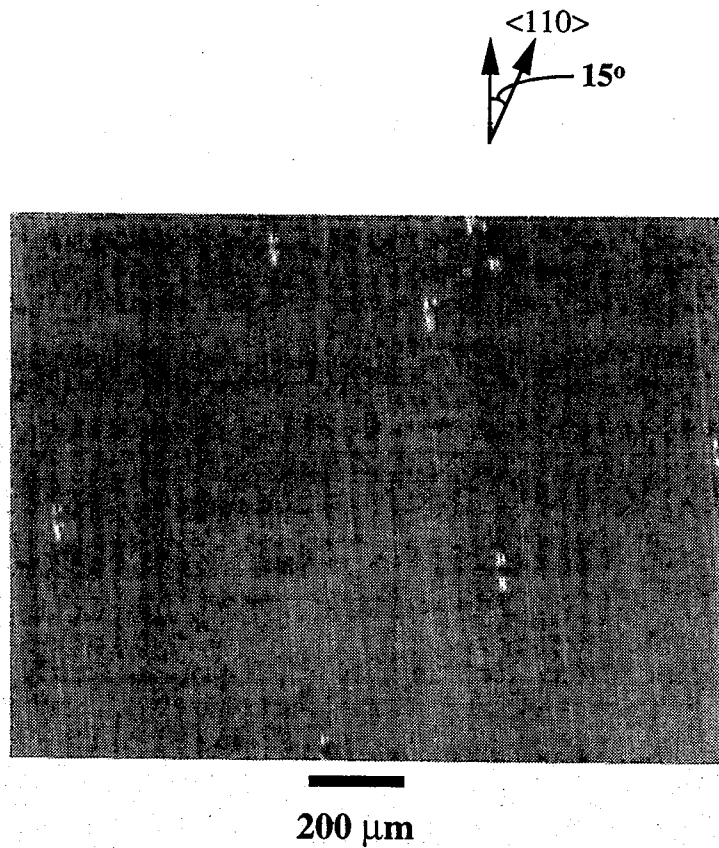


Figure 4.5 : Surface morphology of optical micrograph of ELO film grown on SiO_2 pre-patterned Si substrate with the seed line opening width of $20 \mu\text{m}$ and mask space $50 \mu\text{m}$.

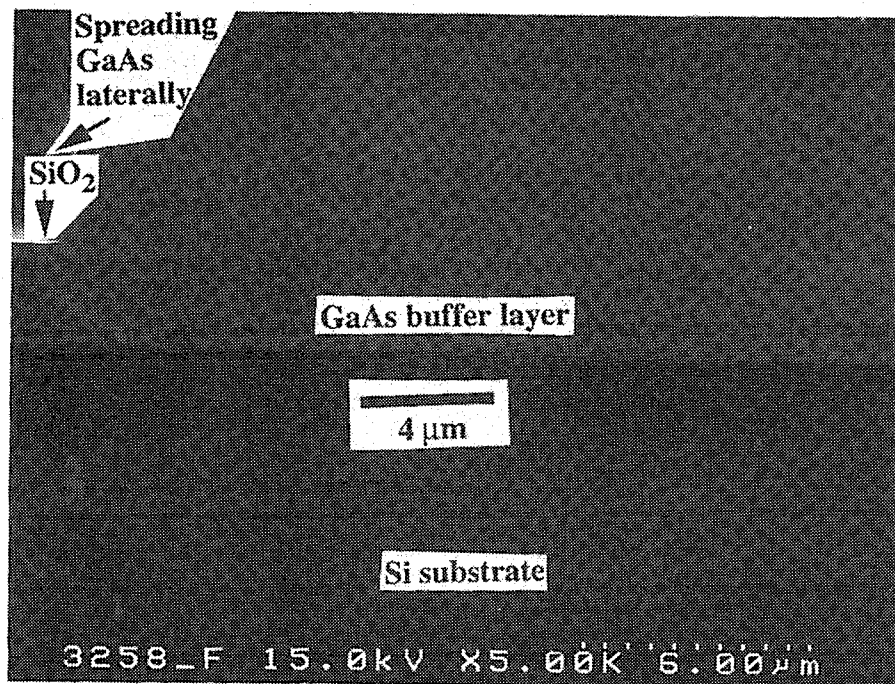


Figure 4.6 : Scanning electron microscope (SEM) image of the cross-section of laterally grown GaAs on Si.

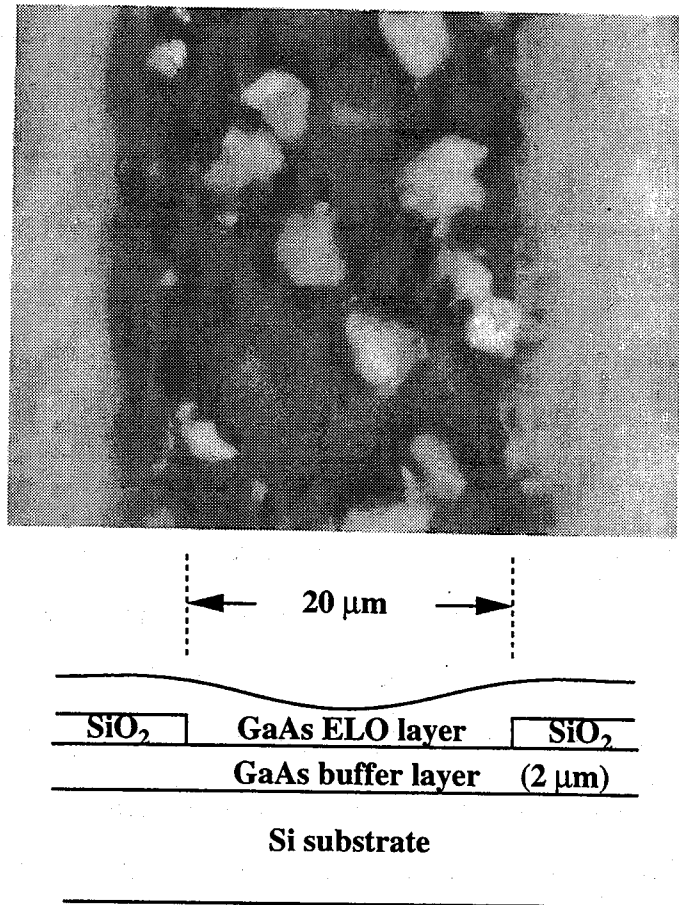


Figure 4.7 : Etch pits of overgrown GaAs epilayer on Si etched by molten KOH etching for 12 minutes at $350\ ^\circ\text{C}$. Etch pits are found only in the line seed region.

free. The density of the etch pits in this region was $\sim 2 \times 10^6 \text{ cm}^{-2}$. The presence of etch pits in the line seed region is originally due to the dislocations propagate from the nucleation layer of GaAs and the ELO layer is nearly dislocation free. So, the observation by etching studies implies that the SiO_2 mask intercepts the dislocation from the nucleation layer of GaAs on Si.

Photoluminescence (PL) spectrum of an ELO layer at RT is shown in Fig. 4.8. This figure shows PL spectra of a conventional GaAs epilayer on GaAs substrate, GaAs epilayer on Si substrate and GaAs ELO layer on Si substrate. The peak wavelength of ELO GaAs and GaAs on Si found shifting from the conventional GaAs epilayer on GaAs (870 nm) to 872.2 nm and 874.6 nm respectively. It is well-known that the bulk thermal expansion coefficient of GaAs is 2.5 % higher than that of Si¹³. Usually growth is carried out at a higher temperature. The strain caused by the lattice mismatch is relaxed by the generation of misfits and the GaAs epilayer is grown essentially stress free. Therefore, at the growth temperature, GaAs and Si maintain their own lattice parameters. When the samples are cooled to room temperature the interfacial atoms will have to maintain the same geometry to minimize the interfacial energy. This forces the GaAs lattice parameter to follow the thermal contraction of the Si lattice parameter, which in turn causes a biaxial tensile strain in the epilayer. The strain in the epilayer is not large enough to cause dislocations but leads to the tetragonal distortion of the GaAs epilayer lattice¹⁴. This strain affects the band gap and valence band degeneracy. As a result the wavelength peak shifts towards the longer wavelength region in case of GaAs/Si. However, the shift of peak wavelength towards the shorter wavelength region, indicates that the ELO technique is also useful to relieve the stress in the epilayer. Further, the stronger PL intensity and narrower full width at half maximum (FWHM) show that the optical quality of the ELO layer is almost as good as that of conventional GaAs epilayer on Si.

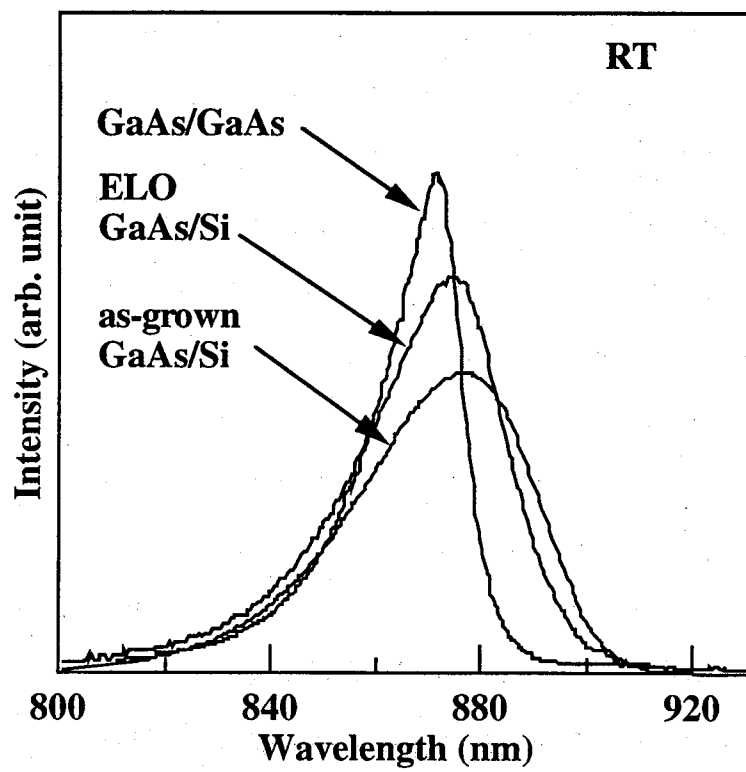


Figure 4.8 : PL spectra of GaAs ELO on Si, as-grown GaAs epilayer on Si and GaAs on GaAs substrate.

4.3.2 Characterization of SQW laser on Si with an ELO layer

Figure 4.9 shows the typical light output vs. injected current characteristics of both the type I and II GaAs SQW laser on an ELO film on Si substrate under continuous wave mode at RT. Type I laser shows a threshold current density of 0.81 kA/cm^2 with an external differential quantum efficiency of 42%, while type II laser shows 1.17 kA/cm^2 and 36% respectively. Figure 4.10 shows the typical emission spectra of the lasers at $I = 1.3 I_{th}$. The type I laser shows the peak wavelength of 854 nm with an half width of 2.2 nm, while for the type II laser these are 861 nm and 2.3 nm respectively. A shift of peak position towards shorter wavelength for the type I laser is may be due to the relaxation of tensile stress in the overgrown layer. The threshold current density found to be lowered than other reported GaAs-based lasers on Si¹⁵⁻¹⁷. This improvement is believed due to the partial filter of dislocation density by the ELO method.

Figure 4.11 shows the results of lifetime test of CW-operated laser carried out at RT, in which the operating current is shown as a function of the time under the constant output power of 1 mW and 2 mW controlled by an automatic power controller. At a constant power of 1 mW, very slow degradation was observed, even after 100 hrs. of operation for the type I laser. But at high power of 2 mW the operating current increase kept the device to operate upto 48 hrs and then a rapid degradation was observed. On the other hand, the type II laser degraded within 5 hrs. at a constant power of 1 mW. The results indicate that the ELO epitaxial growth of GaAs buffer layer is an alternative promising way to minimize the life time degradation. However, the shorter life time at high power operation is due to the generation of secondary dislocation networks in the ELO layer. The source for the secondary defect generation and reduction has to be studied in detail.

Electron beam induced current (EBIC) is an useful method for obtaining qualitative and quantitative information about the dislocation density by the dark

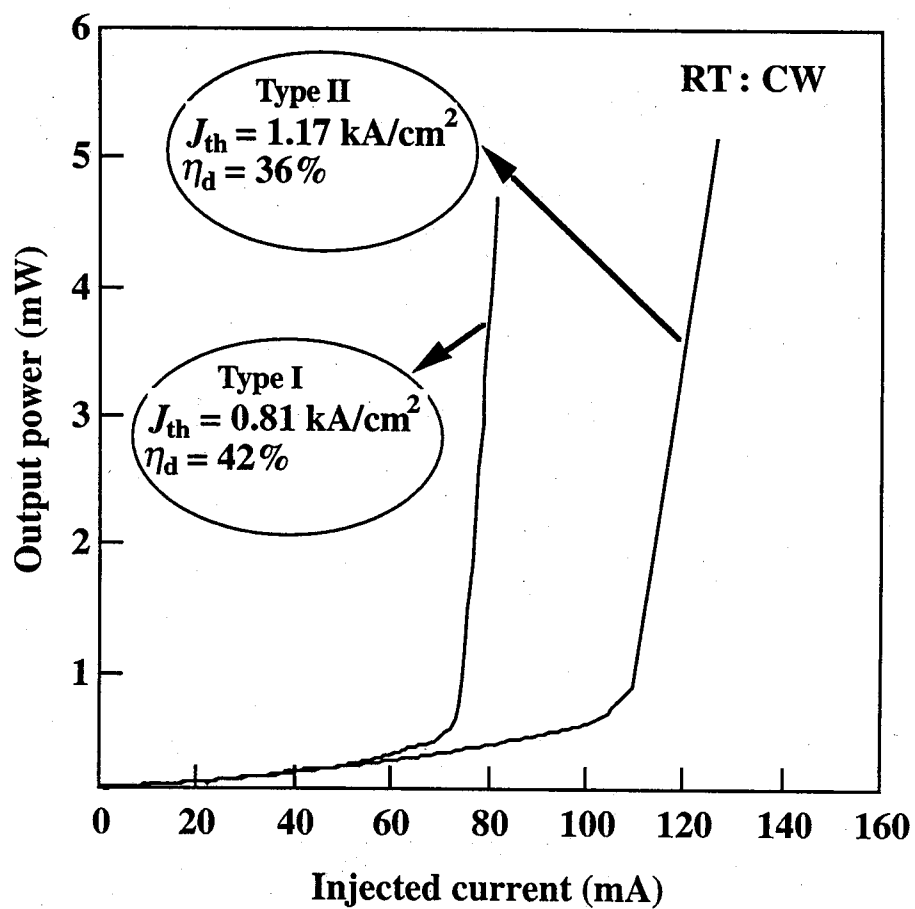


Figure 4.9 : Typical continuous wave light output vs. injected current characteristics of GaAs SQW laser on ELO film on patterned Si substrate.

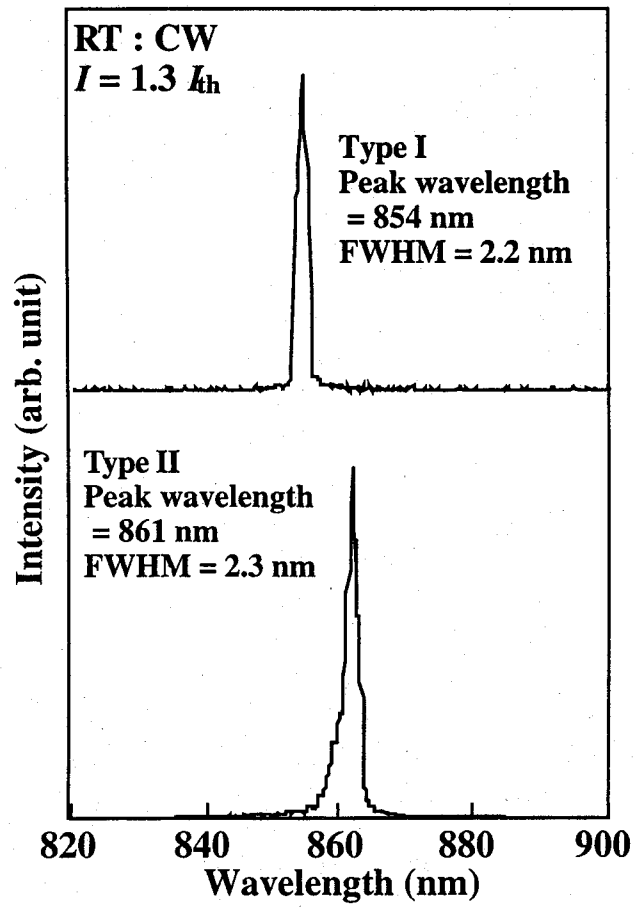


Figure 4.10 : Typical emission spectrum of GaAs SQW laser on micro-channel patterned Si substrate.

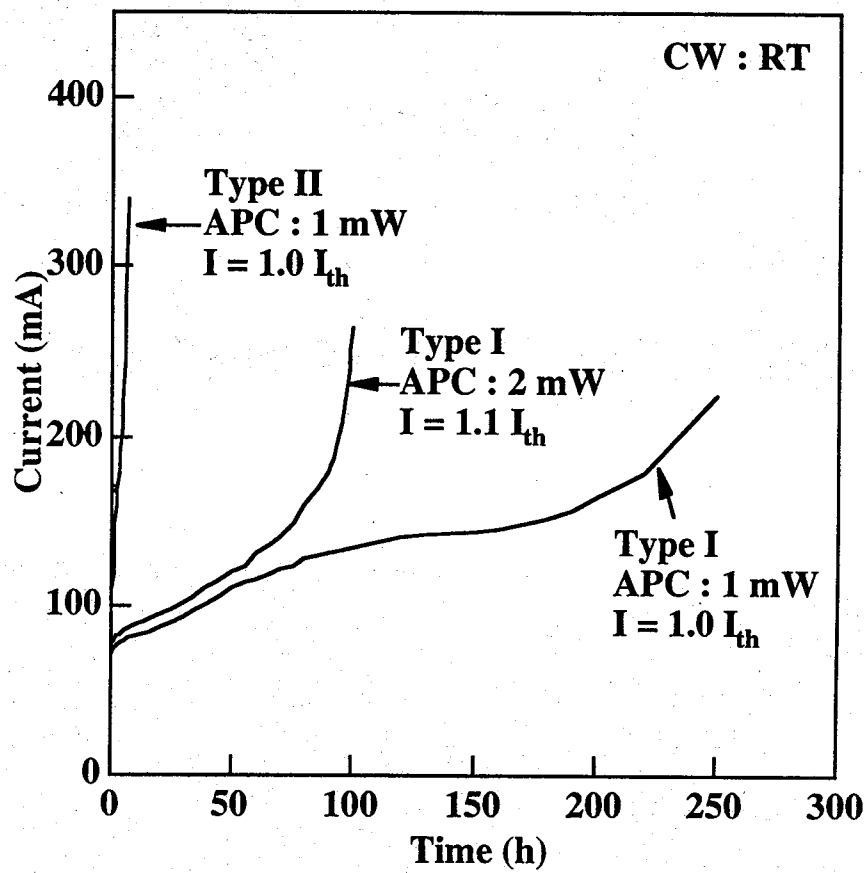
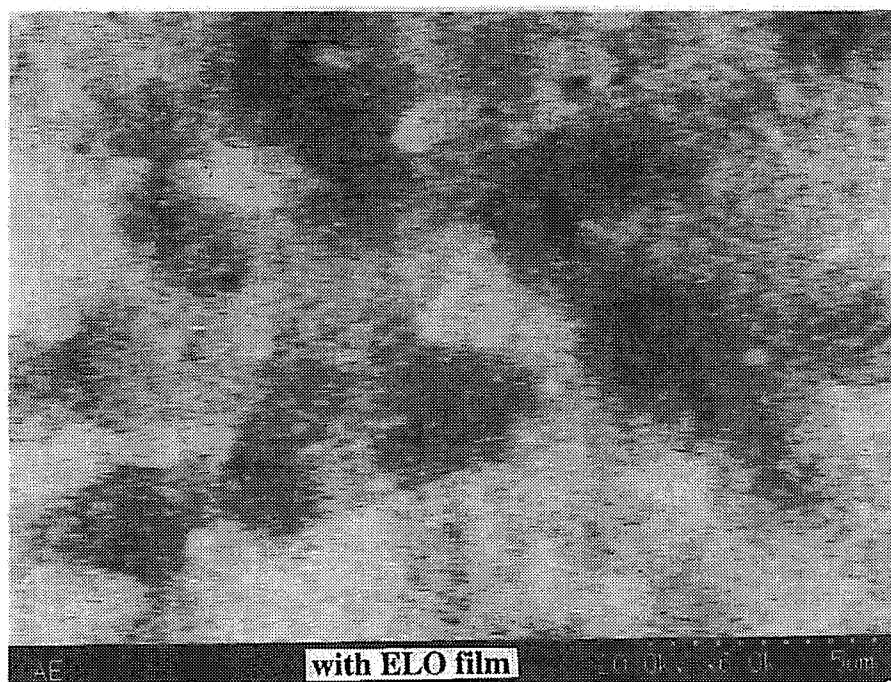
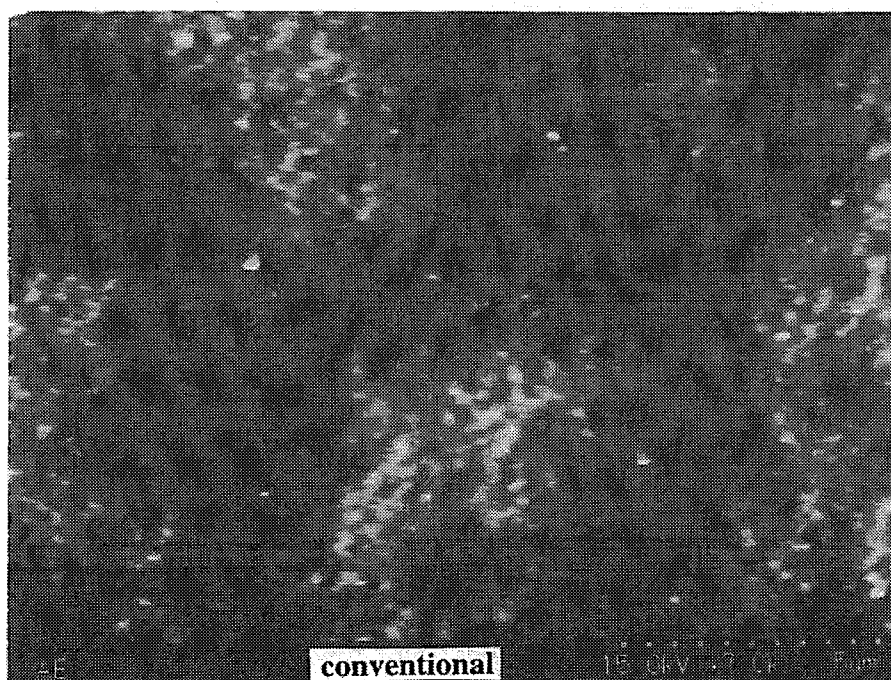


Figure 4.11 : APC aging tests under CW condition at RT for the SQW laser diodes on an ELO film grown on Si substrate.



(a)



(b)

Figures 4.12 : EBIC image of the (a) SQW laser on Si with the ELO film, (b) conventional SQW laser on Si.

spot density (DSD) of EBIC image. In this process, a high-energy electron interacts with a valence band electron, which if sufficient energy is transferred, is excited into the conduction band¹⁸. These high-energy electrons can either be lattice electrons under the influence of a large electric field or, as in the case, incident electrons from outside the specimen. The carriers resulting from an incident electron beam are generated in a finite volume of the material, referred to as the carrier generation volume. The basic of the EBIC technique is that, once injected, these electron-hole pairs subsequently behave in the same way as those injected by other means, such as photogeneration.

The loss of carriers through recombination will clearly lead to a decrease in the current collected by the electric field. This effect is exploited in order to identify crystal defects in semiconductors. Such defects, such as grain boundaries, inclusions and dislocations, are usually associated with enhanced recombination and therefore exhibit EBIC contrast.

Figures 4.12(a) shows the EBIC image of the SQW laser on Si with the ELO film. For a comparison the EBIC image of a conventional SQW laser is shown in Fig. 4.12(b). A considerable difference can be observed in these images when compared to the bright and dark extents. Wider dark spots are observed in the case of conventional SQW laser on Si, while in the case of laser with ELO film the dark spots are narrower. Further, only few regions are darkened in the later case. This result indicates that the ELO film in the laser structure suppressed the formation of dislocation. But, still presence of dark region in the EBIC image is thought to be due to the formation of secondary dislocations from the window regions of the ELO pattern.

4.4 Conclusion

Etch pit free lateral epitaxial layers of GaAs on SiO₂ film were successfully obtained by MOCVD on Si substrate. Etch pit with high density was observed

only in the line seed region. The ELO technique is beneficial not only for the reduction of the dislocation density but also for the relief of the stress, which results in good optical quality of ELO layers. The SQW laser on Si with an ELO layer has CW threshold current density as low as 0.81 kA/cm^2 at 300 K. By using ELO technique the rapid degradation can be suppressed if the formation of secondary dislocation can be minimized by more optimistic way and a longer lifetime of GaAs-based laser on Si substrate can be realized. Therefore, ELO is a promising method to obtain a dislocation-free epilayer as well as high quality laser on Si with longer lifetime.

References

1. A. Y. Cho, and W. C. Ballamy, J. Appl. Phys., **46**, 783 (1975).
2. F. J. Leonberger, C. O. Bozler, R. W. McClelland, and I. Melngailis, Appl. Phys. Lett., **38**, 313 (1981).
3. D. R. Bradbury, T. I. Kamins, and C. W. Tsao, J. Appl. Phys., **55**, 519 (1984).
4. H. Asai, S. Adachi, S. Ando, and K. Oe, J. Appl. Phys., **55**, 3868 (1984).
5. T. Nishinaga, Cryst. Prop. Prep. **31**, 92 (1991).
6. P. O. Hanson, A. Gustafsson, M. Albrecht, H. P. Strunk, and E. Bauser, J. Cryst. Growth, **121**, 790 (1992).
7. H. Shichijo, R. J. Matyi, and A. H. Taddiken, IEDM Tech. Dig., 778 (1987).
8. B. A. Vozak, R. W. McClelland, G. A. Lincoln, A.R. Calawa, D. C. Flanders and M. W. Geis, IEEE Electron Device Lett., **5**, 270 (1984).
9. B. Gerard, X. Marcadet, P. Etienne, D. Pribat, D. Friedrich, J. Eichholz, H. Bernt, H. Hanssen, J-F. Carlin and M. Ilegems, Mat. Res. Soc. Symp. Proc., **535**, 139 (1999).
10. Y. S. Chang, S. Naritsuka, T. Nishinaga, J. Cryst. Growth, **174**, 630 (1997).
11. Y. S. Chang, S. Naritsuka, T. Nishinaga, J. Cryst. Growth, **192**, 18 (1998).
12. S. Naritsuka, T. Nishinaga, M. Tachikawa and H. Mori, J. Cryst. Growth, **211**, 395 (2000).
13. *Thermophysical properties of matter*, vol 13 of TPRC DATA Series, ed. by Y. S. Touloukian, R. K. Kirby, R. E. Taylor and T. Y. R. Lee, (Plenum, New York, 1977).
14. D. S. A. Neuman, H. Zabel, R. Fscher and H. Morkoc, J. Appl. Phys., **61**, 1023 (1987).
15. J. P. van der Ziel, R. D. Dupuis, R. A. Logan, R. M. Mikulyak, C. J. Pinzone and A. Savage, Appl. Phys. Lett., **50**, 454 (1987).

16. H. P. Lee, X. Liu and S. Wang, Appl. Phys. Lett., **56**, 1014 (1990).
17. Z. I. Kazi, T. Egawa, T. Jimbo and M. Umeno, Jpn. J. Appl. Phys., **39**, 3860 (2000).
18. J. I. Goldstein, D. E. Newbury, P. Echlin, D. C. Joy, A. D. Romig, C. E. Lyman, C. Fiori and E. Lifshin, *Scanning Electron Microscopy and X-Ray Microanalysis*, (Plenum Press, New York, 1992).

Summary

This dissertation has described the studies on fabrication and characterization of GaAs-based lasers on Si substrate. The epitaxial growth of GaAs on Si has the serious problem of high dislocation density results from ~4 % lattice mismatch and ~250 % difference in the thermal expansion coefficients between GaAs and Si. This high dislocation density is the main obstacle to realize the high quality devices on Si substrate. For instance, the GaAs-based lasers on Si degrade rapidly due to the reduced minority carriers life time by dislocations. To overcome this problem different approaches in epitaxial growth have been taken until now. Among them two step growth mode, thermal cycle annealing, insertion of strained layer superlattice etc. are well reported. However, the reliable GaAs-based lasers on Si to the same level of GaAs substrate are not yet realized.

Novel approaches like, growth of small dimensional island-like and quantum dot-like (QD-like) active region, epitaxial lateral overgrowth (ELO) are taken in this research studies. In the crystal growth point of view, it seems that these techniques offer unique features to advance the quality devices. The achievement of dislocation-free islands or QD active region leads to the realization of lower threshold current density with higher characteristic temperature and increased gain. Partial interception of dislocation density is possible by using masked substrate in the ELO technique.

Chapter 2 explained the growth of self-formed GaAs islands and fabrication of laser with these islands as an active region on Si substrate by MOCVD. The islands were grown by droplet epitaxy technique. The GaAs islands exhibited a conical shape with heights of 8 nm and diameter of 300 nm with a density of around $1\sim2 \times 10^7 \text{ cm}^{-2}$. Laser with self-formed GaAs islands active regions on Si showed the J_{th} of 5.4 kA/cm² under pulsed condition at 300 K, and J_{th} of 3.9 kA/cm² under CW condition at 100 K. Lasing was observed at wavelengths of

771 nm and 776 nm under pulsed and CW conditions respectively. The operating characteristics such as internal quantum efficiency, internal loss, gain coefficient and transparency current density have been also studied. Further, the island laser on Si shows higher characteristic temperature as well as higher quantum efficiency than those of QW laser on Si. The GaAs island lasers showed longer minority carrier lifetimes than the conventional QW lasers due to the reduction of the dislocation density in the active region.

Chapter 3 described the optimization of the growth conditions of QD by S-K growth mode and the fabrication of lasers on Si substrate with the QD-like active region. Laser with $\text{In}_{0.2}\text{Ga}_{0.8}\text{As}$ QD-like active region showed room temperature CW light emission with a lowest threshold current density of 1.32 kA/cm^2 in our experiment. The shift of the lasing wavelength towards the shorter region of $\text{In}_{0.2}\text{Ga}_{0.8}\text{As}$ QD-like laser in comparison with the reported wavelength for InGaAs QW laser on GaAs was explained as an effect of "In" addition. The laser with $\text{In}_{0.3}\text{Ga}_{0.7}\text{As}$ QD-like active region showed a threshold current density of 1.51 kA/cm^2 under RT pulsed condition. Lasing emission was observed as broad and consists of splitted peaks at a spaced interval due to the nonuniform distribution of the electronic states of the dots. The aging test of this laser revealed that this QD - like lasers are reliable than the QW lasers realized by the same structure on Si.

In chapter 4 the growth of epitaxial lateral overgrowth (ELO) and the fabrication of laser on a ELO film are described. Etch pit free lateral epitaxial layers of GaAs on SiO_2 film were successfully obtained by MOCVD on Si substrate. The SQW laser on Si with an ELO layer has CW threshold current density as low as 0.81 kA/cm^2 at 300 K. By using ELO technique the rapid degradation can be suppressed if the formation of secondary dislocation can be minimized by more optimistic way and a longer lifetime of GaAs-based laser on Si substrate can be realized.

The described investigations on the growth of self assembled GaAs quantum dot like structures and its application to laser diode fabrication, ELO epitaxial growth and its application to laser diode fabrication on silicon pointed out that both approaches in the epitaxial growth mode are promising way to realize longer life time lasers on Si substrate. However, the self assembled quantum dot like structure needs to be optimized in size and distribution in order to get its advantage over laser diode operation, which is limited in our case due to the atmospheric pressure operation of our MOCVD system, which prevents our control over the flow of constituents during growth. In case of ELO technique, formation of secondary dislocation in the ELO epilayer is a main barrier to be overcome. This can be overcome by the proper choice of seed line width and mask width.

Scope for the future work

In this dissertation, the techniques to grow low dimensional islands, QDs and ELO film on Si substrate were described and AlGaAs/GaAs lasers were fabricated using these techniques. According to the results described in chapters 2 and 3, it is assumed that the nonuniformity in the island/dot size is due to the surface curvature or roughness of the GaAs epilayer on Si, which is concerning with the stress due to the difference in the thermal expansion coefficient. This affects the lifetime of the device as well as in device fabrication processes. Though the technique of ELO or selective growth epitaxy on Si substrate suppressing the wafer curvature the optimization is yet to do. One possible way to minimize this problem is the growth of QD on a polished GaAs epilayer on Si. The chemo-mechanical polishing of GaAs epilayer on Si by NaOCl and NH_4OH can provide a lowest surface roughness or curvature. A uniform QD can be expected on such a polished surface and this can improve the device quality as well as lifetime.